The International Journal of Advanced Manufacturing Technology (2018) 97:529–541
https://doi.org/10.1007/s00170-018-1960-7

ORIGINAL ARTICLE

Clinching process for aluminum alloy and carbon fiber-reinforced thermoplastic sheets

P.-C. Lin[1] · J.-W. Lin[1] · G.-X. Li[1]

Received: 20 January 2018 / Accepted: 23 March 2018 / Published online: 5 April 2018

Abstract
This research work used a preheated clinching process for joining aluminum alloy 5052-H32 (Al) and carbon fiber-reinforced thermoplastic (CFRTP) sheets. The preheated and softened CFRTP sheets successfully undergo the excessive compression and bending in the process. Al and CFRTP sheets with a thickness of 1.6 mm thick were used to make Al/CFRTP clinch joints in lap-shear (LS) specimens. Effects of joining force, punch design, and die design on mechanical properties of Al/CFRTP clinch joints were investigated by quasi-static tensile tests and metallographic micrographs. An appropriate setup for the Al/CFRTP clinching process was obtained. Then, a complete fatigue test for Al/CFRTP dissimilar clinching joints was conducted to investigate the fatigue properties of Al/CFRTP clinch joints. The fatigue data were recorded, and the failure modes were analyzed and discussed.

Keywords Clinching · Aluminum alloy 5052-H32 · Carbon fiber-reinforced thermoplastic · Fatigue

1 Introduction

Balancing the requirements between fuel efficiency, exhaust emission, vehicle performance, and manufacturing cost are always critical to the automotive industry. Therefore, the concept of car body design gradually shifts from the light-weight design to right-weight design, which optimizes the strength, mass, and cost of car body. According to this advanced design concept, many hybrid car body designs, which are made of steels (Fe), aluminums (Al), and even carbon fiber-reinforced plastic (CFRP), have been proposed in the industry [1, 2].

In production lines, a critical point for manufacturing hybrid car bodies is the joining technology for dissimilar materials, such as aluminum-to-steel (Al/Fe), aluminum-to-CFRP (Al/CFRP), and aluminum-to-glass fiber-reinforced plastic (Al/GFRP). For Al/Fe dissimilar joining, currently, many automotive production lines prefer self-piercing riveting (SPR), friction stir spot welding (FSSW), clinching, and resistance spot welding (RSW) due to their short processing time and reliable mechanical performance [3–10]. On the other hand, the requirements for Al/CFRP dissimilar joining are not much in the past but increasing rapidly in the recent days due to strict emission standards. For example, BMW AG recently uses SPR, flow drill screwing (FDS), and adhesive bonding in the production lines of i-series and 7-series sedans to make joints between aluminum and CFRP components [11–13]. However, the disadvantages of these joining processes are quite significant. For example, the additional weight and cost of SPR and FDS can be quite high when their number achieves more than hundreds. The adhesive bonding usually degrades fast when it is exposed under ultraviolet light. In addition, the reliability of adhesive bonding is questionable under service conditions.

In order to overcome the above problems for Al/CFRP dissimilar joining, many alternate joining processes, such as clinching [14–24], laser joining [25, 26], friction spot joining (FSpJ) [27–29], and ultrasonic spot welding (USW) [30–32], are proposed as reviewed by Pramanik et al. [33]. Among these joining processes, the clinching process is considered as a promising candidate for Al/CFRP dissimilar joining since it provides good mechanical performance, short processing time, and low operation cost. For example, Huang et al. [14] proposed a hybrid joining process, a combination of clinching and adhesive bonding, to join carbon fiber-reinforced thermosetplastic (CFRTsP) and aluminum sheets. The processing temperature was increased to 100 °C for 10 s to

✉ P.-C. Lin
imepcl@ccu.edu.tw

[1] Advanced Institute of Manufacturing with High-tech Innovations and Department of Mechanical Engineering, National Chung-Cheng University, Chia-Yi 62102, Taiwan

improve the ductility of CFRTsP sheets. However, they found that the preheating process cannot soften the CFRTsP sheet. Therefore, the small plastic deformation (mechanical interlock) provides relatively low contributions on the joint strength compared to the adhesive bonding. On the other hand, Lee et al. [15–17] proposed a modified clinching process, called hole-clinching, to make Al/Fe, Al/CFRP, and Fe/CFRP joints to avoid the ductility problem of CFRTsP sheets. Unlike the tradition clinching process, the hole-clinching process needs to drill a hole in the lower sheet before clinching. The interlock of the hole-clinching joint is formed by the undercut of the upper sheet and the hole of the lower sheet. In their research works, a design procedure for the punch, hole, and die, the critical dimensions of the hole-clinching process, was proposed. A finite element model of the hole-clinching process was developed to predict the interlock shape, joining force, and defect location of joints. The effects of the punch shape on the mechanical properties of hole-clinch joints were investigated through tensile shear tests and experimental observations. They indicated that the alignment between hole, punch, and die is very critical to the quality of the joint. Note that although the mechanical performance of hole-clinching joints is quite good, the requirements of predrilled holes and precise alignment for this process may not be available for the mass production line.

On the other hand, Lambiase and Ilio [18] and Lambiase [19, 20] used another modified clinching process to join thermoplastic polymer and aluminum sheets. The polymer sheets were heated by an air flow of 400 °C for more than 5 s before clinching. They reported that the heated and softened polymer sheet can successfully undergo the clinching process. Also, the joining force has significant effects on the mechanical interlock inside the joint.

Lambiase and Ko [21] and Lambiase et al. [22] further studied the suitability of the traditional clinching process to make Al/CFRTsP and Al/GFRP dissimilar joints, respectively. Several commonly used punch and die designs were considered. They reported that the joints made by the round split die and large punch diameter can provide relatively large mechanical interlock and good mechanical performance compared to the other punches and dies. However, the CFRTsP or GFRP sheet at the bottom of the joint is severely damaged or penetrated due to excessive bending in the clinching process. Note that these defects or holes may significantly degrade the fatigue performance of clinch joints.

In order to further improve the performance of clinch joints, Lambiase and Ko [23] proposed a modified clinching process, called two-step clinching, to reshape the undercut of Al/CFRTsP clinch joints. They found that the second clinching step can largely increase the undercut size and the joint strength. Lambiase and Paoletti [24] proposed a friction-assisted clinching process to improve the ductility of aluminum sheets and reduce the joining force. The effects of processing parameters on the quality and strength of clinch joints were studied. Although the strength of clinch joints was improved by the two clinching processes, similar defects or holes were still found at the bottom of clinch joints.

In the previous research works, the low ductility of CFRTsP sheets is the main reason for the defects of Al/CFRTsP clinch joints. In order to overcome this problem, the carbon fiber-reinforced thermoplastic (CFRTP) sheets and the preheating process are considered in this study based on the concept reported in Lambiase [20]. Then, the effects of the joining force, die design, and punch diameter on the mechanical properties of clinch joints between aluminum alloy 5052-H32 (Al) and CFRTP sheets are investigated. Three punches and five dies are taken to make clinch joints in lap-shear (LS) specimens. Quasi-static tensile tests and metallographic micrograph observations are conducted. An appropriate process setup for the Al/CFRTP clinching process is then obtained to conduct a complete fatigue test. The fatigue data and failure modes of Al/CFRTP clinch joints are then recorded and discussed.

2 Experiments

In this study, aluminum alloy 5052-H32 (Al) and CFRTP sheets with a thickness of 1.6 mm were used to make joints. Note that the aluminum alloy 5052 and CFRTP sheets considered here since they are commonly used in the automotive industry. Unlike commonly used CFRTsP sheets, CFRTP sheets can be softened by heating. Also, recycling CFRTP sheets is relatively easy and cheap. This fact is important for satisfying the increasingly strict environmental laws. The corresponding thicknesses of Al and CFRTP sheets were determined according to one of the specifications for body panels. The CFRTP sheets composed of 16 prepreg layers with cross lay-up [0°/90°/90°/0°/0°/0°/90°/90°/0°/0°/0°/90°/90°/0°/0°/0°/90°/90°/0°] were supplied by TOPKEY Inc., as shown in Fig. 1. Each prepreg layer has an average thickness of 0.1 mm, and the carbon fiber has a diameter of 22 μm. The mechanical properties of Al and CFRTP sheets are listed in Table 1.

Three circular punches, P1 to P3, and five circular dies, D1 to D5, were used. The important dimensions of the punch and die are defined in Fig. 2. In Fig. 2a, the probe diameter and probe length are denoted as D_p and L_p, respectively. The shoulder diameter is denoted as D_s. In Fig. 2b, the die diameter and die depth are denoted as D_d and d_d, respectively. The groove radius, groove width, and groove depth are denoted as r_g, w_g, and d_g, respectively. The dimensions of the punches and dies are listed in Table 2. The punch and die were installed inside a pneumatic and hydraulic press machine, ARC-10T, from APMATIC Corp., as shown in Fig. 3.

In order to evaluate the mechanical performance of Al/CFRTP clinch joints, LS specimens made by using two

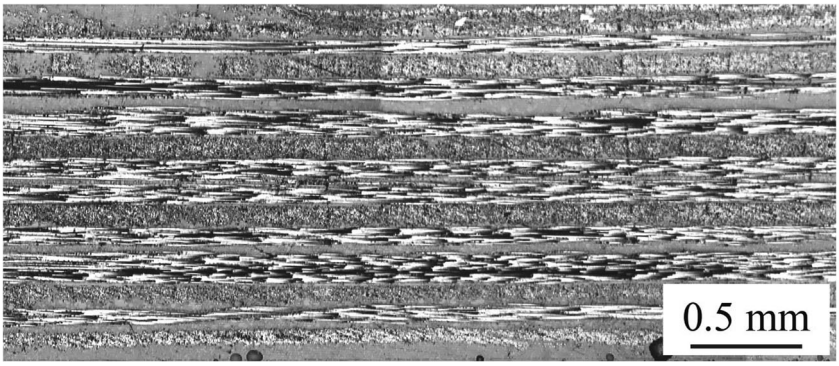

Fig. 1 A cross-sectional micrograph of a CFRTP sheet

25.4 mm by 101.6 mm sheets with a 25.4 mm by 25.4 mm overlap area were used. The LS specimen is designed based on the standard of AWS C1.1M/C1.1:2000, as shown in Fig. 4. Two doublers were adopted in the tests for LS specimens to align the applied load at the initial realignment stage. Note that the Al and CFRTP sheets were taken as the upper and lower sheets, respectively.

In quasi-static tensile tests, LS specimens were tested by a universal testing machine at a monotonic displacement rate of 5.0 mm/min. The failure loads were recorded. The average failure load obtained from three to five tested specimens was then used as a reference to determine the load ranges of fatigue tests. In fatigue tests, the specimens were tested at a load ratio R of 0.1 and a frequency of 10 Hz. The experimental plane and corresponding processing parameters used in the following are listed in Table 3.

3 Al/CFRTP clinching process

Conventionally, the clinching process is conducted at room temperature. Thus, the sheet metals should have sufficient ductility to undergo the extremely large plastic deformation during the process. Otherwise, the clinch joint may be fractured or cracked. In this study, AA5052-H32 (Al) and CFRTP sheets were used to make Al/CFRTP dissimilar clinch joints. The ductility of Al sheets is sufficient but that of CFRTP sheets is quite poor at the room temperature, as listed in Table 1. In order to overcome this critical problem, an additional preheating process for CFRTP sheets was taken to improve their ductility and formability, as suggested in Lambiase [20]. Note that the CFRTP sheet used here becomes soft and ductile when the temperature is above 85 °C. Figure 5 schematically shows the modified clinching process for Al/CFRTP dissimilar clinch joints. First, a CFRTP sheet was heated to 100 °C by a CORNING PC-420D hot plate and then stacked on an Al sheet inside a fixture immediately, as shown in Fig. 5a. Second, the two sheets were clamped tightly by a holder and then pressed into a die by a punch, as shown in Fig. 5b. The two sheets were deformed plastically as two button structures. Third, the two button structures were continuously squeezed into the groove and a strong mechanical interlock was made between them, as shown in Fig. 5c. Finally, the punch was drawn out and then an Al/CFRTP dissimilar clinch joint was made, as shown in Fig. 5d. Note that the whole process including the installation and clinching should be done within 10 s. If the punch, die, and sheets are warmed up before clinching by induction heating, the preheating process can be removed and the whole processing time can be even shorter.

4 Results and discussion

As listed in Table 3, a preliminary study of the clinching process for Al and CFRTP sheets is first conducted to understand the typical joining conditions of clinch joints. Next, the contributions of the joining force, groove size, die depth, and punch diameter on the failure loads and joint geometries of Al/CFRTP dissimilar clinch joints in LS specimens are studied. Once an appropriate process setup for the clinching process is obtained, a complete fatigue test for Al/CFRTP clinch joints is conducted.

4.1 Preliminary study

Figure 6 shows cross-sectional micrographs of Al/CFRTP dissimilar clinch joints with various joining conditions. Figure 6a shows a clinch joint having good interlock between the inner (Al) and outer (CFRTP) buttons. The clinch joint is made by P1

Table 1 Mechanical properties of aluminum alloy 5052-H32 and CFRTP sheets

	Elastic modulus (GPa)	Tensile strength (MPa)	Elongation (%)	Density (g/cm^3)
Al5052-H32	70.3	193	12	2.68
CFRTP	250	4680	1.9	1.81

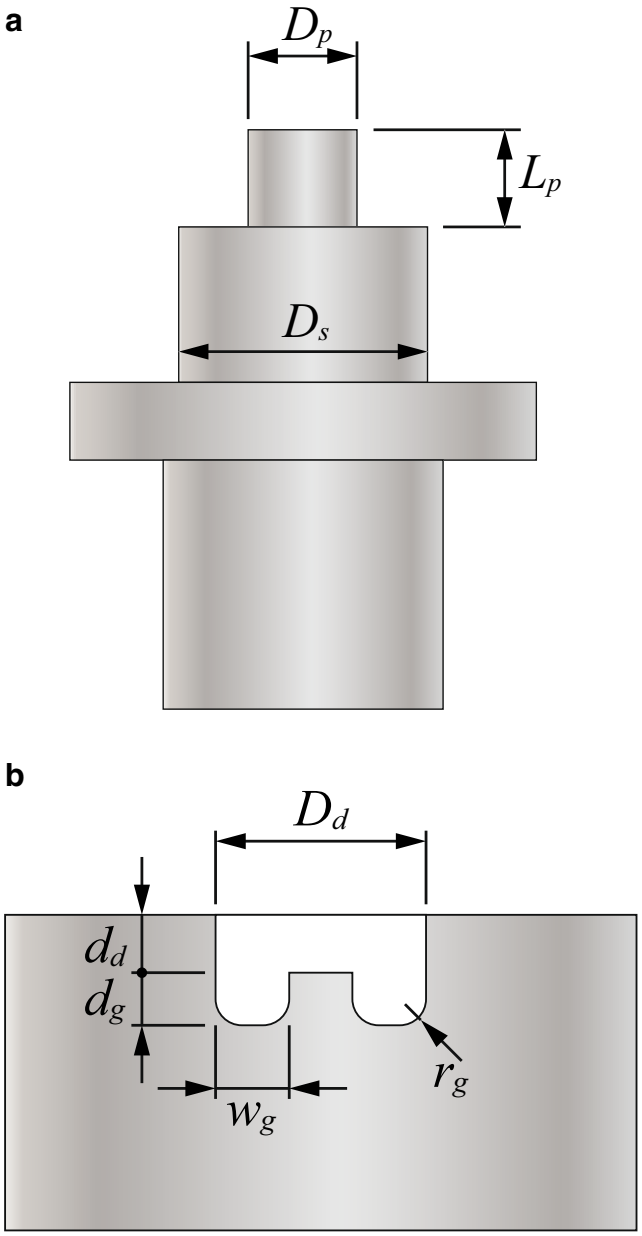

Fig. 2 Schematics of **a** a circular punch and **b** a circular die with a groove

(D_p : 7.0 mm) punch and D1 (d_d : 1.1/w_g : 1.0/d_g : 0.5 mm) die under a joining force of 44 kN. Note that the critical dimensions of the punch and die are listed here, while their remaining dimensions can be found in Table 2. The neck of the inner button and the undercut of the outer button can be seen clearly. Two notches, marked by arrows, between the upper and lower sheets can be seen near the circumference of the inner and outer buttons. Note that in the inner button, no crack or defect can be found. However, in the outer button, several types of defects can be seen at the corner and bottom, such as delamination, crack, and debonding. These defects are probably caused by excessive bending or compression during the clinching process. Similar problems can be seen in Fig. 6b, c. It should be noted that the preheating process can soften the matrix of the CFRTP sheet, but not the carbon fibers inside. Therefore, when the softened CFRTP sheet is bent or compressed severely, the carbon fibers inside may be fractured or debonded. The effects of defects on the mechanical performance of Al/CFRTP dissimilar clinch joints will be discussed later.

Table 2 Detailed dimensions of circular punches, P1 to P3, and circular dies, D1 to D5

	P1	P2	P3		
D_p	7.0	6.5	6.0		
L_p	6.25				
D_s	16.0				
Unit: mm					
	D1	D2	D3	D4	D5
D_d	10.0				
d_d	1.1	1.1	1.1	0.7	0.4
r_g	0.5				
w_g	1.0	2.0	1.0	1.0	1.0
d_g	0.5	0.5	0.75	0.5	0.5
Unit: mm					

Figure 6b shows a clinch joint having poor interlock between the inner and outer buttons. The clinch joint is made by P1 (D_p : 7.0 mm) punch and D1 (d_d : 1.1/w_g : 1.0/d_g : 0.5 mm)

Fig. 3 Pneumatic and hydraulic press machine, ARC-10T, from APMATIC Corp.

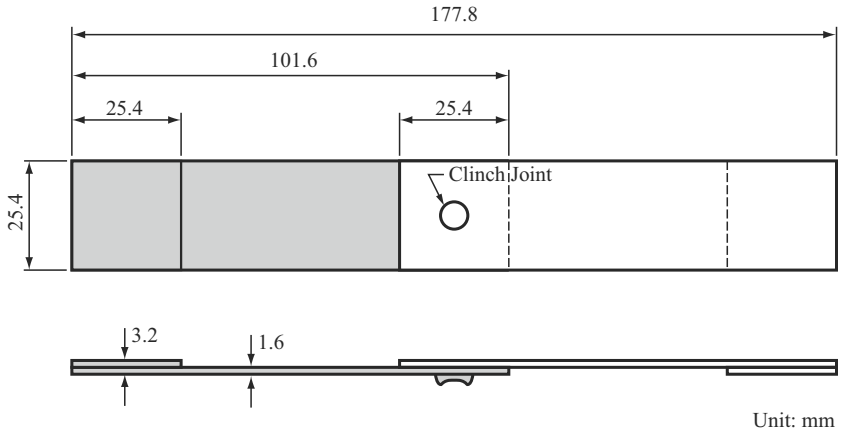

Fig. 4 Schematics of a LS specimen with an Al/CFRTP joint

die under a joining force of 30 kN. Compared to the joint in Fig. 6a, the poor interlock may be caused by the relatively low joining force. In Fig. 6b, the neck of the inner button and the undercut of the outer button cannot be seen clearly. In general, a clinch joint with poor interlock usually has relatively poor mechanical performance. Figure 6c shows a clinch joint having neck fracture in the inner button. The clinch joint is made by P1 (D_p : 7.0 mm) punch and D2 (d_d : 1.1/w_g : 2.0/d_g : 0.5 mm) die under a joining force of 61 kN. Compared to the joint in Fig. 6a, the cracks in the necks may be caused by the relatively high joining force and improper die design. In general, when a clinch joint has fracture or large crack at the neck or nearby region in the inner button, it is taken as a failed joint since it may not have any strength and is not available in the industry. The corresponding processing setup, including joining force, tool design, and die design, will not be considered in the following. Figure 6d, e shows top and back views of an Al/CFRTP dissimilar clinch joint with good interlock, respectively. As shown in the top view, a circular hole is located at the center of the overlap area. In the back view, a circular cylinder surrounded by a ring can be seen at the center of the overlap area. Several superficial cracks, marked by arrows, can be seen on the surface. These defects correspond to those shown in Fig. 6a.

4.2 Joining force effects

In contrast to other joining machines, the press machine in Fig. 3 for clinching process is relatively simple. The most important operation parameter of the machine is the joining force. Figure 7 shows the failure load vs. joining force for Al/CFRTP dissimilar clinch joints in LS specimens made by P1 (D_p : 7.0 mm) punch and D1 (d_d : 1.1/w_g : 1.0/d_g : 0.5 mm) die. In Fig. 7, when the joining force increases from 34 to 50 kN, the failure load increases gradually and then achieves the maximum. When the joining force continuously increases, the failure load slightly decreases and then drops to zero. As discussed earlier, whenever a clinch joint has crack or fracture in the inner button (Al), the joint quality is not available in the industry and therefore, the failure load is given as zero here.

Figure 8 shows cross-sectional micrographs of Al/CFRTP clinch joints made by P1 (D_p : 7.0 mm) punch and D1 (d_d : 1.1/w_g : 1.0/d_g : 0.5 mm) die under joining forces of 34, 44, and 61 kN, respectively. As shown in Fig. 8, the effects of the joining force on the interlock structure of clinch joints are quite significant. When the joining force is small, the neck of the inner button is thick and the undercut of the outer button is very small, as shown in Fig. 8a and as listed in Table 4. This joint has a poor interlock with a low failure load, as shown in Fig. 7, and a button separation failure mode. When the joining force increases, the neck becomes thinner and the undercut becomes larger, as shown in Fig. 8b and as listed in Table 4. This joint has a good interlock with a higher failure load, as shown in Fig. 7, and a button separation failure mode. However, when the joining force continuously increases to 61 kN, the neck becomes very thin and the undercut becomes very large, as listed in Table 4. At the same time, many large cracks and fractures can be seen in the outer button, as shown

Table 3 Experimental plan and corresponding processing parameters

	Preliminary study	Joining force	Groove size	Die depth	Punch diameter	Fatigue test
Joining force	34–65 kN	34–65 kN	34–65 kN	34–65 kN	34–65 kN	61 kN
Punch	P1	P1	P1	P1	P1, P2, P3	P1
Die	D1, D2	D1	D1, D2, D3	D1, D4, D5	D4	D4

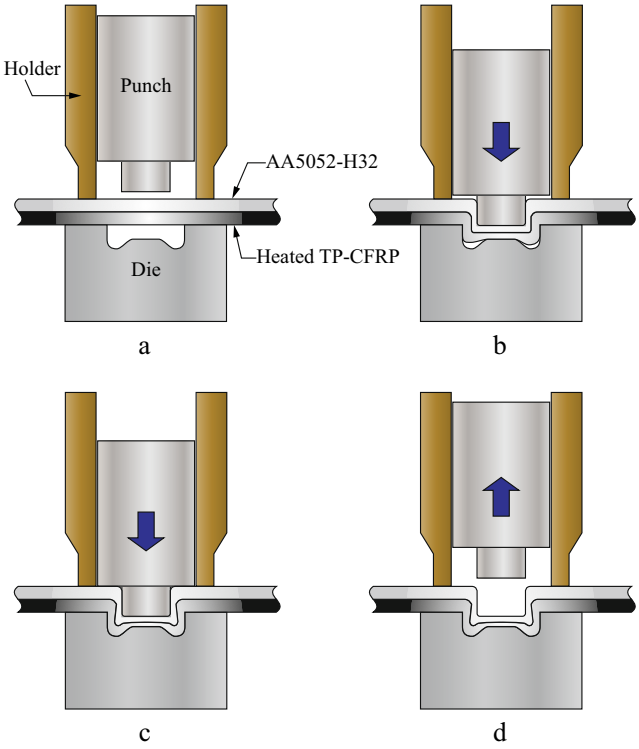

Fig. 5 Schematics of the Al/CFRTP clinching process. **a** Clamping. **b** Punching. **c** Interlocking. **d** Drawing out

in Fig. 8c. Although this joint still has a good interlock, its failure load slightly decreases and its failure mode transfers to neck fracture.

As shown in Figs. 7 and 8, when the joining force is low, the interlock structure of clinch joints is poor and the corresponding failure load is poor as well. On the other hand, when the joining force is too large, the button neck is cracked or fractured and the failure load may be zero. Finally, the clinch joint with a joining force of 50 kN has a good interlock and a good failure load.

4.3 Groove size effects

In this section, the relationships between the groove size, a critical feature of the die, and the mechanical performance of Al/CFRTP dissimilar clinch joints were studied. Three dies, D1, D2, and D3, with different groove designs were used. Note that when the punch squeezes a clinch joint, the groove provides an additional space for the materials at the joint bottom, guides the material flow to appropriate locations, and finally forms a good interlock for the joint. As listed in Table 2, D1 die has the original dimensions, D2 die has a larger groove width w_g, and D3 die has a larger groove depth d_g. The groove width of D2 and the groove depth of D3 in fact provide similar volume increase for the grooves of the two dies. With the help of larger groove volumes, more materials can flow into the groove and probably provides a better interlock for joints.

Figure 9 shows the failure load vs. the joining force for Al/CFRTP dissimilar clinch joints in LS specimens made by D1, D2, and D3 dies and P1 punch. For joints made by D1 die (original), the failure loads are identical to those in Fig. 7. For joints made by D2 die (wider groove), when the joining force increases from 34 to 44 kN, the failure loads are all equal to zero since these joints are neck fractured during the process. When the joining force continuously increases, the failure load gradually increases. For joints made by D3 die (deeper groove), when the joining force increases from 34 to 50 kN, the failure load increases and then slightly decreases. When the joining force continuously increases, the failure load gradually increases again. As shown in Fig. 9, D1 die still has the maximum failure load among three dies and is therefore selected as the reference die for the following process.

Figure 10 shows cross-sectional micrographs of Al/CFRTP clinch joints made by D1, D2, and D3 dies with P1 punch under a joining force of 44 kN, respectively. In Fig. 10a, the joint made by D1 die has a good interlock structure and a good failure load, as shown in Fig. 9. In Fig. 10b, the joint made by D2 die has fractured necks during the process. Therefore, its failure load is given as zero in Fig. 9. Note that when the

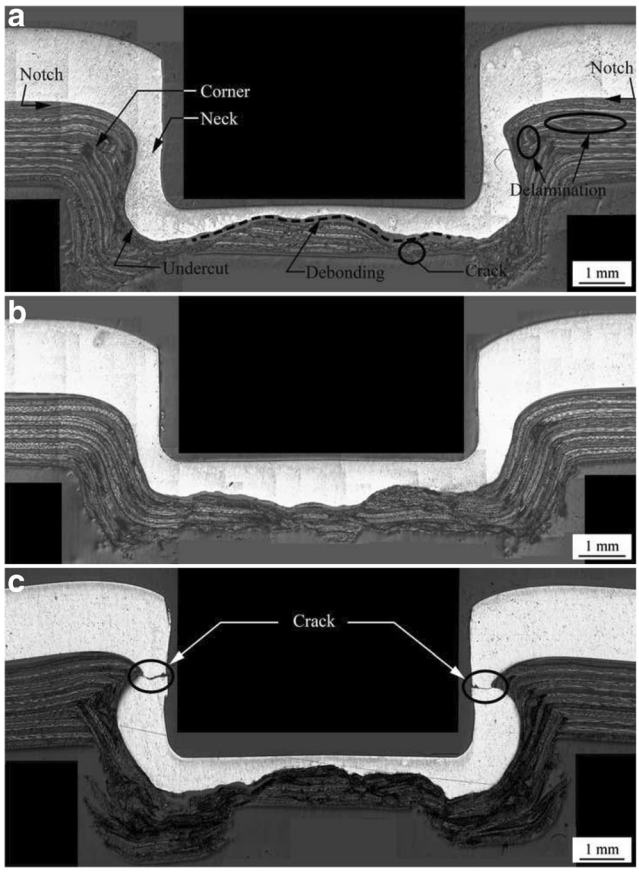

Fig. 6 Cross-sectional micrographs of Al/CFRTP clinch joints with **a** good interlock, **b** poor interlock, and **c** neck fracture. **d** Top view and **e** back view of an Al/CFRTP clinch joint

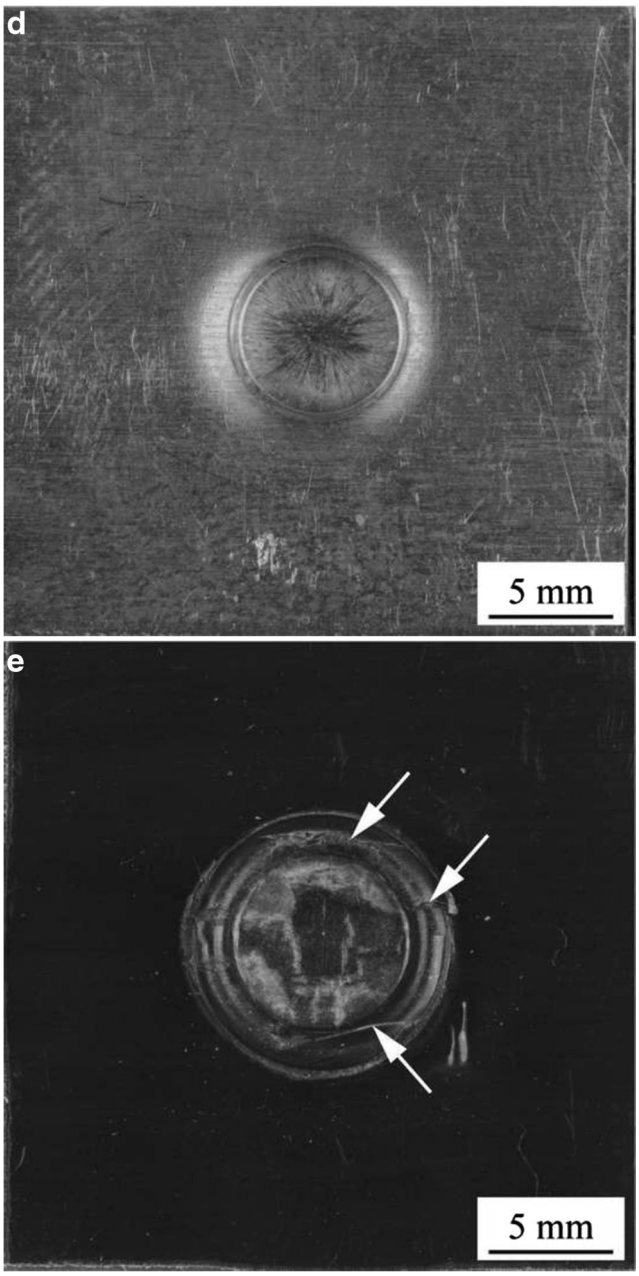

Fig. 6 (continued)

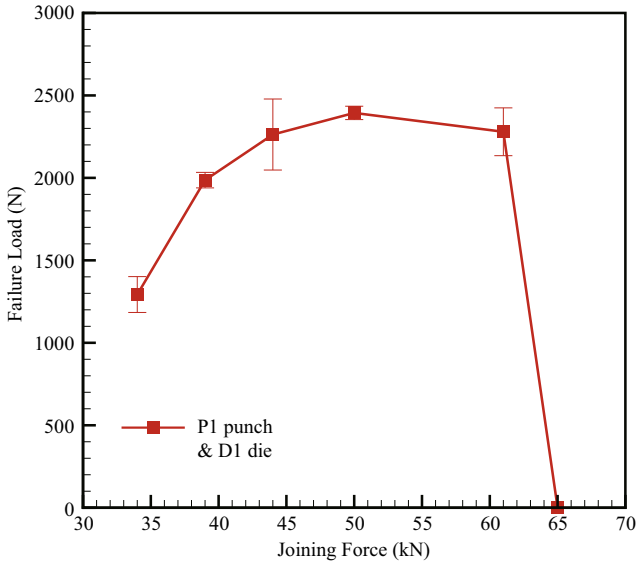

Fig. 7 Failure load vs. joining force for Al/CFRTP dissimilar clinch joints in LS specimens made by P1 punch (D_p : 7.0 mm) and D1 die (d_d : 1.1/w_g : 1.0/d_g : 0.5 mm)

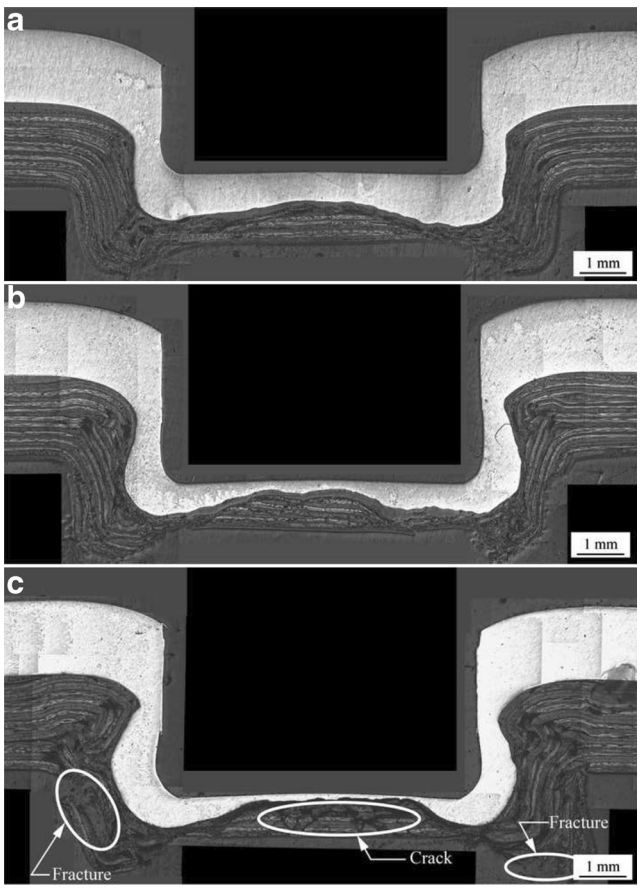

Fig. 8 Cross-sectional micrographs of Al/CFRTP clinch joints made by P1 punch (D_p : 7.0 mm) and D1 die (d_d : 1.1/w_g : 1.0/d_g : 0.5 mm) under joining forces of **a** 34, **b** 44, and **c** 61 kN

punch presses the sheets into D2 die, the wider groove provides a larger space for the materials of the inner and outer buttons to flow downwards and outwards. A large undercut can be seen at the bottom of the joint. However, the total amount of materials pressed by the same punch is nearly the same. Thus, the neck of the inner button is fractured probably because too much material flows into the groove and joint bottom. In Fig. 10c, the joint is made by D3 die and has a deep undercut in the outer button. Note that when the punch presses the sheets into D3 die, the deeper groove provides a larger space as well. However, the amount of material flows downwards into the groove is not as much as that in Fig. 10b

Table 4 Neck and undercut dimensions of the clinching joints in Fig. 8

Joining force (kN)	Right neck (mm)	Left neck (mm)	Right undercut (mm)	Left undercut (mm)
34	0.59	0.54	0	0
44	0.52	0.52	0.27	0.35
61	0.48	0.45	0.62	0.42

probably because the groove width is smaller than that of D2 die. Therefore, the neck of the inner button just becomes longer and thinner, which results in a median failure load as shown in Fig. 9.

It should be noted that when the joining force continuously increases to 50 kN or more, the joints made by D2 and D3 dies both provide higher failure loads, as shown in Fig. 9. The possible reason is that when the joining force increases, the space between the punch and die becomes smaller and the material flowing downwards becomes less. This fact results in an interlock structure with thicker button necks, which provide larger failure loads.

4.4 Die depth effects

In this section, the relationships between the die depth, the other critical feature of the die, and the mechanical performance of Al/CFRTP dissimilar joints were studied. Note that when the punch presses the sheets into the die, the die depth determines the amount of materials flowing into the die, the length of the button wall, and the thickness of the button neck. In general, a smaller die depth provides shorter button walls and thicker button necks, which may further improve the joint strength. Here, three dies, D1, D4, and D5, with different die depths were used. As listed in Table 2, D1 die has the original dimensions, D4 die has a die depth d_d of 0.7 mm, and D5 die has a die depth d_d of 0.4 mm. The die depths of D4 and D5 dies are smaller than D1 die.

Figure 11 shows the failure load vs. the joining force for Al/CFRTP dissimilar clinch joints in LS specimens made by P1 punch and D1, D4, and D5 dies. For joints made by D1 die (original), the failure loads are obtained from those in Fig. 7. For joints made by D4 die, when the joining force increases from 34 to 61 kN, the failure load increases rapidly at the beginning, and then gradually achieves the maximum. When the joining force continuously increases, the failure load

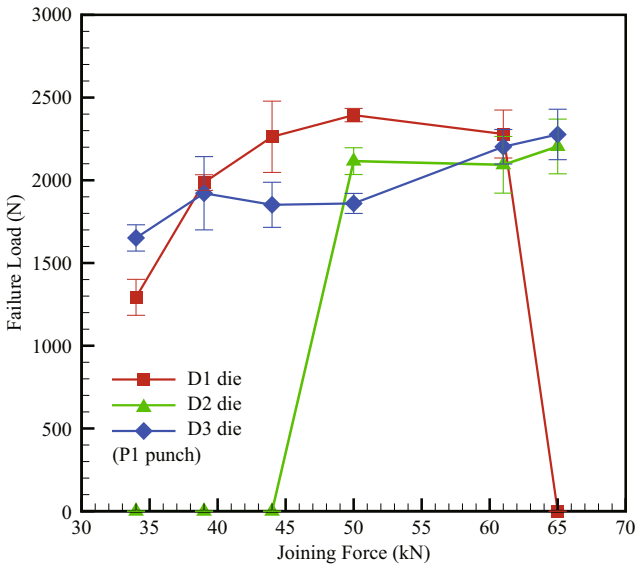

Fig. 9 Failure load vs. joining force for Al/CFRTP dissimilar clinch joints in LS specimens made by D1 (d_d : 1.1/w_g : 1.0/d_g : 0.5 mm), D2 (d_d : 1.1/w_g : 2.0/d_g : 0.5 mm), and D3 (d_d : 1.1/w_g : 1.0/d_g : 0.75 mm) dies with P1 punch (D_p : 7.0 mm)

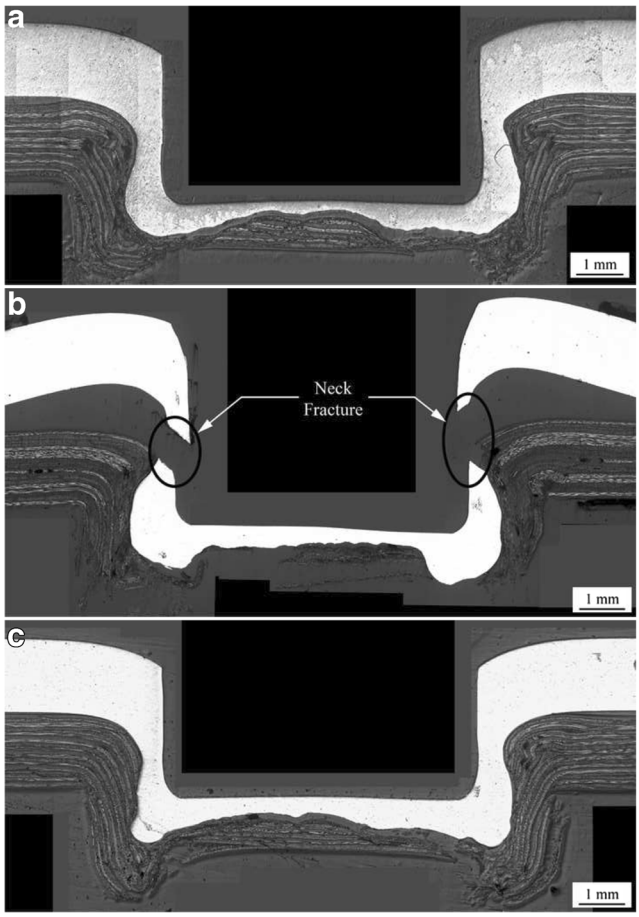

Fig. 10 Cross-sectional micrographs of Al/CFRTP clinch joints made by **a** D1 (d_d : 1.1/w_g : 1.0/d_g : 0.5 mm), **b** D2 (d_d : 1.1/w_g : 2.0/d_g : 0.5 mm), and **c** D3 (d_d : 1.1/w_g : 1.0/d_g : 0.75 mm) dies with P1 punch (D_p : 7.0 mm) under a joining force of 44 kN

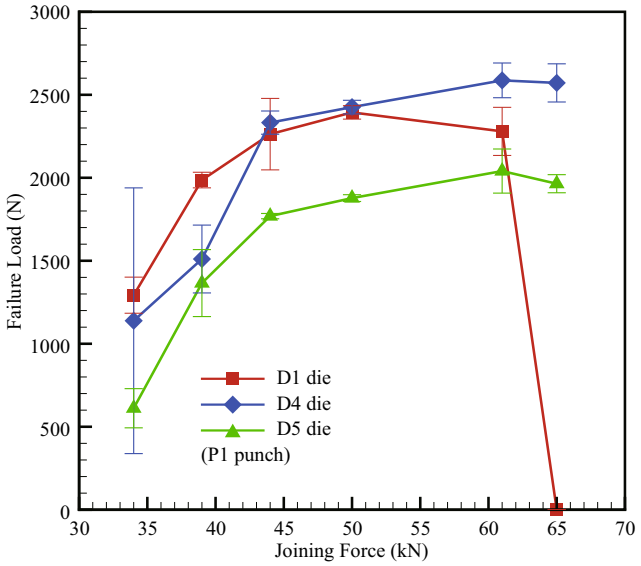

Fig. 11 Failure load vs. joining force for Al/CFRTP dissimilar clinch joints in LS specimens made by D1 (d_d : 1.1/w_g : 1.0/d_g : 0.5 mm), D4 (d_d : 0.7/w_g : 1.0/d_g : 0.5 mm), and D5 (d_d : 0.4/w_g : 1.0/d_g : 0.5 mm) dies with P1 punch (D_p : 7.0 mm)

slightly decreases. For joints made by D5 die, the general trend is similar to that made by D4 die. As shown in Fig. 11, D4 die has the maximum failure load among three dies and is selected as the reference die for the following process.

Figure 12 shows cross-sectional micrographs of Al/CFRTP clinch joints made by D1, D4, and D5 dies with P1 punch under a joining force of 61 kN, respectively. In Fig. 12a, the joint made by D1 die is taken as a reference. Note that several defects of crack and fracture can be seen at the bottom of the outer button. In Fig. 12b, the joint made by D4 die has thicker button necks, shorter button walls, and similar undercuts than that made by D1 die. Note that two large defects of delamination can be seen at the shoulder of the outer button. Several defects of crack and debonding can be seen at the bottom of the outer button. Although the more defects can be found in the outer button, the failure load of the joint is still higher than that made by D1 die. A possible reason is that the joint is failed in the inner button not the outer one. The other reason is that thicker button necks with similar undercuts improve the joint strength significantly. In Fig. 12c, the joint made by D5 die has even thicker button necks, shorter button walls than those made by D1 and D4 dies. However, the undercut of the joint becomes quite small probably due to a limited constraint from the shallow die. Without sufficient undercut, the joints made by D5 die have relatively low joint strength, as shown in Fig. 11.

4.5 Punch diameter effects

In this section, the relationships between the punch diameter, the critical feature of the punch, and the mechanical performance of Al/CFRTP dissimilar joints were studied. Note that when the punch presses the sheets into the die, the punch diameter determines the diameter of the inner button and the total thickness of the joint wall, including the inner and outer buttons. In general, a smaller punch diameter gives a smaller inner button, thicker joint walls, a thinner joint bottom, and larger undercuts. The reason is that for given applied load, the average pressure applied to the joint increases when the punch diameter decreases. Thus, due to larger pressure applied to the joint bottom, the joint bottom becomes thinner and the materials there flow outwards to the grooves and then enlarge the undercuts. Here, three punches, P1, P2, and P3, with D4 die were used. As listed in Table 2, P1 punch has the original dimensions, P2 punch has a diameter D_p of 6.5 mm, and P3 punch has a diameter D_p of 6.0 mm. The diameters of P2 and P3 punches are smaller than P1 punch.

Figure 13 shows the failure load vs. the joining force for Al/CFRTP dissimilar clinch joints in LS specimens made by P1, P2, and P3 punches with D4 die. For joints made by P1 punch with D4 die, the failure loads are obtained from those in Fig. 11. For joints made by P2 punch, when the joining force increases from 34 to 61 kN, the failure load decreases at the

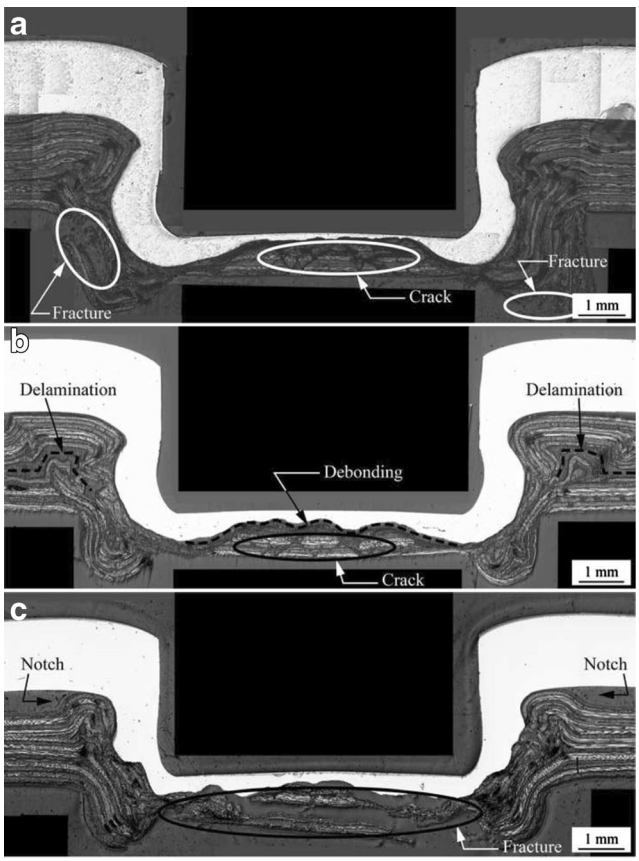

Fig. 12 Cross-sectional micrographs of Al/CFRTP clinch joints made by **a** D1 (d_d : 1.1/w_g : 1.0/d_g : 0.5 mm), **b** D4 (d_d : 0.7/w_g : 1.0/d_g : 0.5 mm), and **c** D5 (d_d : 0.4/w_g : 1.0/d_g : 0.5 mm) dies with P1 punch (D_p : 7.0 mm) under a joining force of 61 kN

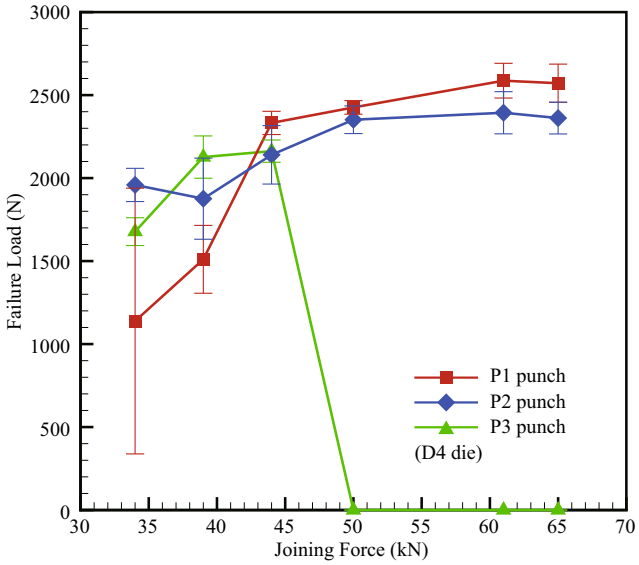

Fig. 13 Failure load vs. joining force for Al/CFRTP dissimilar clinch joints in LS specimens made by P1 (D_p : 7.0 mm), P2 (D_p : 6.5 mm), and P3 (D_p : 6.0 mm) punches with D4 (d_d : 0.4/w_g : 1.0/d_g : 0.5 mm) die

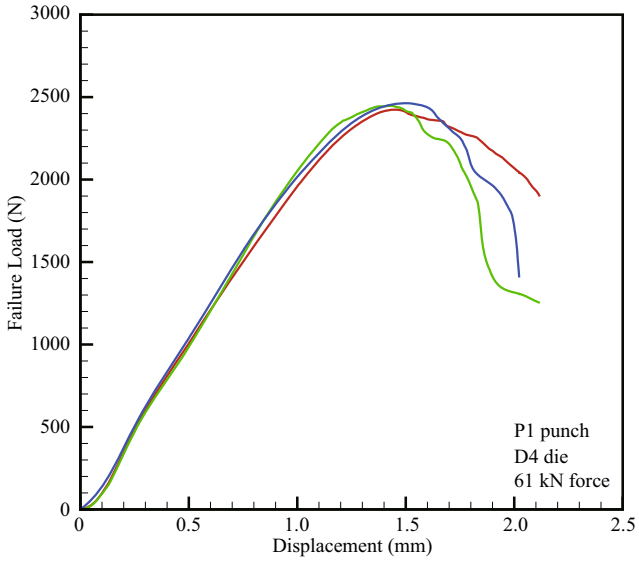

Fig. 14 Force-displacement curves of Al/CFRTP clinch joints made by P1 (D_p : 7.0 mm) and D4 (d_d : 0.4/w_g : 1.0/d_g : 0.5 mm) die under a joining force of 61 kN

beginning and then gradually increases to the maximum. When the joining force continuously increases, the failure load slightly decreases. For joints made by P3 punch, the general trend is quite different to those for joints made by P1 and P2 punches. When the joining force increases from 34 to 44 kN, the failure load gradually increases to the maximum and then drops to zero due to button separation. Note that when the joining force exceeds 44 kN, the bottom of the outer button is fully fractured, the mechanical interlock between the inner and outer buttons is released, and then the inner and outer buttons are separated easily. In Fig. 13, the joints made by P1 punch provide the maximum failure load among three punches and is selected as the reference punch for the following fatigue tests.

Based on the results shown in Fig. 13, the processing parameters of P1 (D_p : 7.0 mm) punch, D4 (d_d : 0.4/w_g : 1.0/d_g : 0.5 mm) die, and 61-kN joining force are taken as the reference parameters for the following fatigue tests. Figure 14 shows three force-displacement curves of Al/CFRTP clinch joints made by the above processing parameters. The average failure load of 2587 N and the elongation of 2.1 mm are comparable with the results reported in Lambiase and Ko [23].

Figure 15 shows cross-sectional micrographs of Al/CFRTP clinch joints made by P1, P2, and P3 punches with D4 die under a joining force of 44 kN, respectively. Note that the joining force of 44 kN is selected here since this is the maximum applied force for the joint made by P3 punch. In Fig. 15a, the joint made by P1 punch is taken as a reference. No significant defect can be seen in the outer button except two large gaps or notches between the upper and lower sheets located at the shoulder of the joint. In Fig. 15b, the joint made by P2 punch has a small inner button with similar shape compared to that made by P1 punch. A fracture defect can be found at the bottom of the outer button. This fact can explain that the failure load of this joint is slightly lower than that of the joint made by P1 punch, as shown in Fig. 13. In

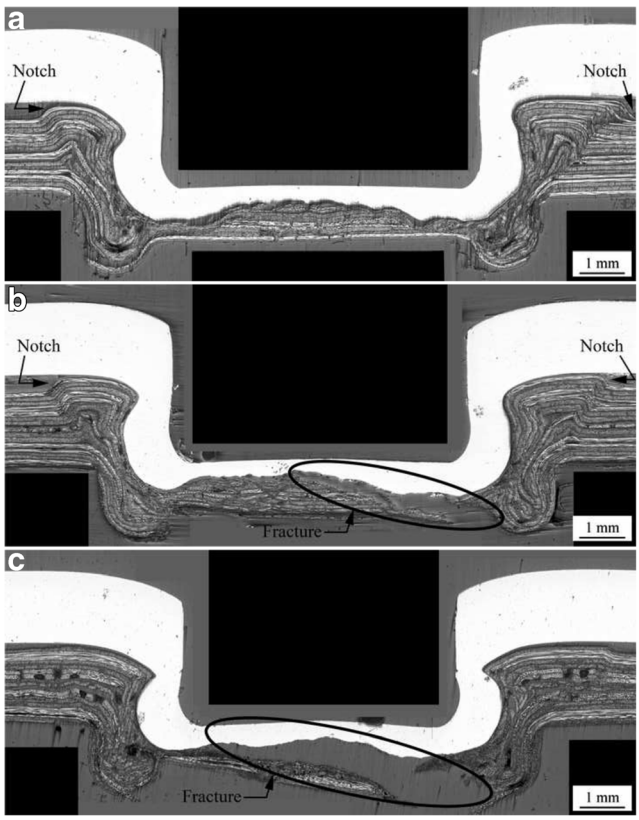

Fig. 15 Cross-sectional micrographs of Al/CFRTP clinch joints made by **a** P1 (D_p : 7.0 mm), **b** P2 (D_p : 6.5 mm), and **c** P3 (D_p : 6.0 mm) punches with D4 (d_d : 0.4/w_g : 1.0/d_g : 0.5 mm) die under a joining force of 44 kN

Fig. 15c, the joint made by P3 punch has a smaller inner button, thinner button necks, and larger undercuts than those made by P1 and P2 punches. A significant fracture defect can be seen at the bottom of the outer button. In Fig. 13, this joint provides similar failure load as that made by P2 punch probably because it has better interlock structure but smaller inner button. Note that once the bottom of the outer button is totally fractured and separated due to overload, the mechanical interlock between the inner and outer buttons will be fully released.

4.6 Fatigue test results

Figure 16 shows the fatigue data of Al/CFRTP clinch joints made by P1 punch and D4 die under joining force of 61 kN in LS specimens. The cyclic loads have maximum values vary from 80 to 30% of the average failure load, 2587 N. As shown in Fig. 16, two failure modes can be seen, including button separation and neck fracture. It is interesting that the joints failed in the button separation failure mode are subjected to higher load ranges with lower fatigue lives. On the other hand, the joints failed in neck fracture are subjected to lower load ranges with higher fatigue lives. Therefore, in this study, the former and latter regions are denoted as the low-cycle and high-cycle conditions, respectively, based on their failure modes. Next, the micrographs and pictures of the failed specimens will be studied and discussed.

Figure 17a shows a cross-sectional micrograph of a failed Al/CFRTP clinch joint in a LS specimen under low-cycle conditions. The applied load range is 1863 N, and the fatigue life is 1782 cycles. The thick arrows indicate the directions of applied loads. As shown in Fig. 17a, the right notch first

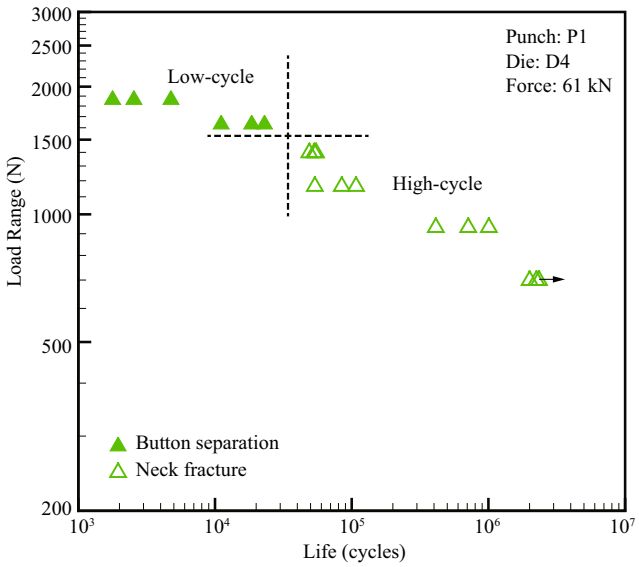

Fig. 16 Load range vs. fatigue life for Al/CFRTP clinch joints in LS specimens made by P1 (D_p : 7.0 mm) punch with D4 (d_d : 0.4/w_g : 1.0/d_g : 0.5 mm) die under joining force of 61 kN

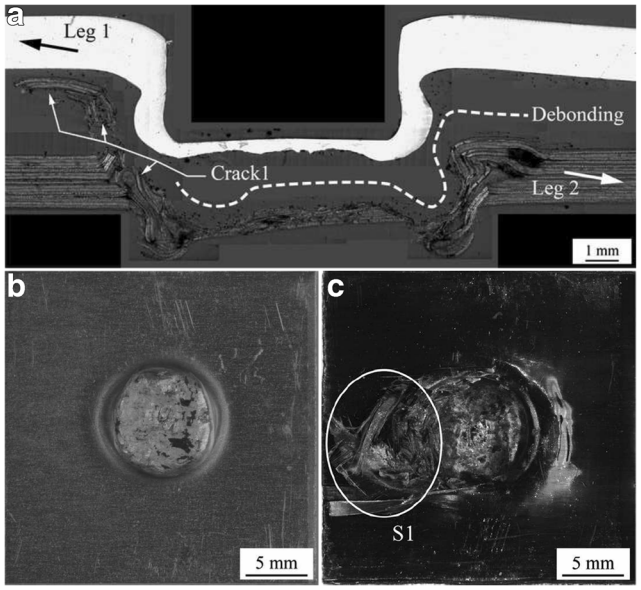

Fig. 17 **a** A cross-sectional micrograph of a failed Al/CFRTP clinch joint in LS specimens under low-cycle conditions. The applied load range is 1863 N, and the fatigue life is 1728 cycles. **b** The back view of the inner button and **c** the top view of the outer button of another failed Al/CFRTP clinch joint

advances towards the left hand side along the interface between the inner and outer buttons and becomes a debonding failure. A fatigue crack, crack 1, then initiates from the surface of the left undercut in the outer button (CFRTP) and then propagates into the corner towards the upper surface. Once

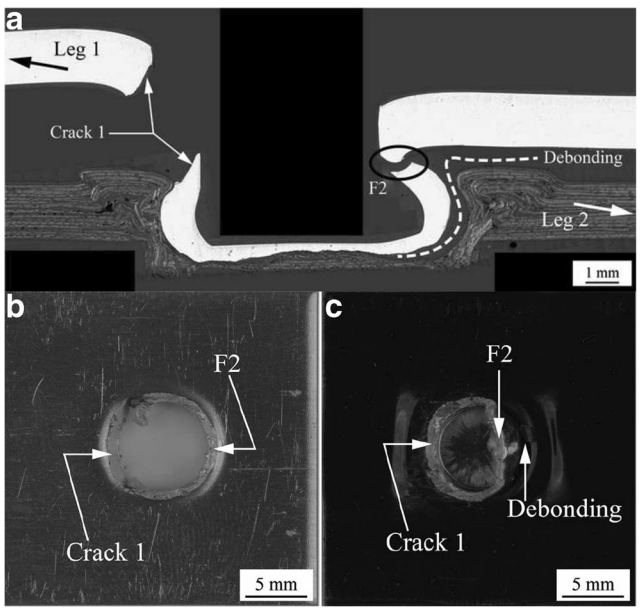

Fig. 18 **a** A cross-sectional micrograph of a failed Al/CFRTP clinch joint in a LS specimen under high-cycle conditions. The applied load range is 1397 N, and the fatigue life is 54,830 cycles. **b** The back view of the upper sheet and **c** the top view of the lower sheet of another failed Al/CFRTP clinch joint

the corner of the outer button is fractured, the interlock between the inner and outer buttons is totally released. The button separation failure mode can be seen. Note that since crack 1 grows through the left corner of the outer button, the crack or delamination at this region, as shown in Fig. 12b, may deteriorate the fatigue lives of joints failed in the button separation. Figure 17b shows the back view of the inner button of a failed Al/CFRTP clinch joint. No crack or damage can be seen on the inner button. Figure 17c shows the top view of the outer button of a failed Al/CFRTP clinch joint. The fracture surface on the left side of the outer button corresponds to fatigue crack 1 in Fig. 17a.

Figure 18a shows a cross-sectional micrograph of a failed Al/CFRTP clinch joint in a LS specimen under high-cycle conditions. The applied load range is 1397 N, and the fatigue life is 54,830 cycles. As shown in Fig. 18a, the right notch first advances towards the left hand side along the interface between the inner and outer buttons and becomes a debonding failure, which stops growing near the right undercut. A fatigue crack, crack 1, then initiates from the surface of the left neck in the inner button (Al). Crack 1 then propagates through the button neck and transforms to a circumferential crack. Finally, the neck of the inner button is fractured and the upper and lower sheets are separated. The neck fracture failure mode can be seen. Note that since crack 1 grows through the neck of the inner button, the cracks or defects in the outer button, as shown in Fig. 12, have no effects on the fatigue lives of joints failed in the neck fracture. Figure 18b shows the back view of a failed Al/CFRP clinch joint in the upper sheet. The annular fracture surface corresponds to the fatigue crack 1 and circumferential crack in Fig. 18a. Figure 18c shows the top view of a failed Al/CFRP clinch joint in the lower sheet. The annular fracture surface corresponds to fatigue crack 1 and circumferential crack in Fig. 18a as well.

5 Conclusions

This work used a preheated clinching process for joining aluminum alloy 5052-H32 and CFRTP sheets. Aluminum and CFRTP sheets with a thickness of 1.6 mm was used to make joints in LS specimens. A parametric study on the punch diameter, die geometry, and joining force was conducted. Three punches and five dies were used. The process was then analyzed through quasi-static tensile tests, optical micrographs, and fatigue testing. The following major conclusions were obtained:

1. The heated and softened CFRTP sheets are feasible for the Al/CFRTP clinching process since they have sufficient ductility to undergo the severe compression and bending in the process.
2. In the Al/CFRTP clinching process, when the joining force increases, the button neck thickness gradually decreases while the undercut size increases.
3. The groove width and groove depth of the die have significant effects on the undercut shape and size of Al/CFRTP clinch joints.
4. When the die depth decreases, the button neck thickness gradually increases while the undercut remains similar size and then shrinks to a very small size and a weird shape.
5. When the punch diameter decreases, the joint diameter, button neck thickness, and the corresponding failure load of clinch joints decreases.
6. With the help of the failure loads and micrographs of Al/CFRTP clinch joints made under various conditions, an appropriate processing setup, including P1 punch and D4 die with a joining force of 61 kN, was obtained.
7. A complete fatigue test for Al/CFRTP clinch joints in LS specimens was conducted. The fatigue data were recorded. Two failure modes, button separation and neck fracture, were found in the failed clinch joints under low-cycle and high-cycle conditions, respectively.

Acknowledgements The authors greatly appreciate the financial supports from the Ministry of Science and Technology, Taiwan, under Grant Nos. 104-2221-E-194-033 and 105-2221-E-194-020-MY2.

References

1. Carle D, Blount G (1999) The suitability of aluminium as an alternative material for car bodies. Mater Des 20:267–272
2. Sakurai T (2008) The latest trends in aluminum alloy sheets for automotive body panels. Kobelco Technol Rev 28:22–28
3. Tran V-X, Pan J (2010) Fatigue behavior of dissimilar spot friction welds in lap-shear and cross-tension specimens of aluminum and steel sheets. Int J Fatigue 32:1167–1179
4. Sun YF, Fujii H, Takaki N, Okitsu Y (2013) Microstructure and mechanical properties of dissimilar al alloy/steel joints prepared by a flat spot friction stir welding technique. Mater Des 47:350–357
5. Lin P-C, Liao P-S, Su Z-M, Aoh J-N (2014) Mechanical properties and failure modes of friction stir clinch joints between 6061-T6 aluminum and S45C steel sheets. In: Proceedings of the 10th international symposium of friction stir welding, Beijing, China, May 20–22, 2014
6. Lee C-J, Kim J-Y, Lee S-K, Ko D-C, Kim B-M (2010) Parametric study on mechanical clinching process for joining aluminum alloy and high-strength steel sheets. J Mech Sci Technol 24:123–126
7. Abe Y, Mori K, Kato T (2012) Joining of high strength steel and aluminium alloy sheets by mechanical clinching with dies for control of metal flow. J Mater Process Technol 212:884–889
8. Sun X, Khaleel MA (2005) Performance optimization of self-piercing rivets through analytical rivet strength estimation. J Manu Process 7:83–93
9. Sun X, Stephens EV, Khaleel MA (2007) Fatigue behaviors of self-piercing rivets joining similar and dissimilar sheet metals. Int J Fatigue 29:370–386
10. Zhang W, Sun D, Han L, Gao W, Qiu X (2011) Characterization of intermetallic compounds in dissimilar material resistance spot

welded joint of high strength steel and aluminum alloy. ISIJ Int 51: 1870–1877
11. Starke J (2017) Carbon composites in automotive structural applications. http://www.eucia.eu/userfiles/files/Starke-Eucia%202016-V4-Druck%20b.pdf
12. Ueda M, Miyake S, Hasegawa H, Hirano Y (2012) Instantaneous mechanical fastening of quasi-isotropic CFRP laminates by a self-piercing rivet. Compos Struct 94:3388–3393
13. Franco GD, Fratini L, Pasta A (2013) Analysis of the mechanical performance of hybrid (SPR/bonded) single-lap joints between CFRP panels and aluminum blanks. Int J Adhes Adhes 41:24–32
14. Huang Z, Sugiyama S, Yanagimoto J (2013) Hybrid joining process for carbon fiber reinforced thermosetting plastic and metallic thin sheets by chemical bonding and plastic deformation. J Mater Process Technol 213:1864–1874
15. Lee SH, Lee CJ, Kim BH, Ahn MS, Kim BM, Ko DC (2014) Effect of tool shape on hole clinching for CFRP with steel and aluminum alloy sheet. Key Eng Mater 622:476–483
16. Lee CJ, Lee SH, Lee JM, Kim BH, Kim BM, Ko DC (2014) Design of hole-clinching process for joining CFRP and aluminum alloy sheet. Int J Precis Eng Manuf 15:1151–1157
17. Lee CJ, Lee SH, Lee JM, Kim BH, Kim BM, Ko DC (2014) Influence of tool shape on hole clinching for carbon fiber-reinforced plastic and SPRC440. Adv Mech Eng 6:810864
18. Lambiase F, Ilio A (2015) Mechanical clinching of metal-polymer joints. J Mater Process Technol 215:12–19
19. Lambiase F (2015) Mechanical behaviour of polymer-metal hybrid joints produced by clinching using different tools. Mater Des 87: 606–618
20. Lambiase F (2015) Joinability of different thermoplastic polymers with aluminium AA6082 sheets by mechanical clinching. Int J Adv Manuf Technol 80:1995–2026
21. Lambiase F, Ko D-C (2016) Feasibility of mechanical clinching for joining aluminum AA6082-T6 and carbon fiber reinforced polymer sheets. Mater Des 107:341–352
22. Lambiase F, Durante M, Ilio AD (2016) Fast joining of aluminum sheets with glass fiber reinforced polymer (GFRP) by mechanical clinching. J Mater Process Technol 236:241–251
23. Lambiase F, Ko D-C (2017) Two-steps clinching of aluminum and carbon fiber reinforced polymer sheets. Compos Struct 164:180–188
24. Lambiase F, Paoletti A (2018) Friction-assisted clinching of aluminum and CFRP sheets. J Manuf Process 31:812–822
25. Jung K-W, Kawahito Y, Katayama S (2013) Laser direct joining of CFRP to metal or engineering plastic. Trans JWRI 42:5–8
26. Katayama S, Kawahito Y (2014) Laser joining carbon fiber-reinforced plastic to stainless steel. Ind Laser Solut 29:22–24
27. Amancio-Filho ST, Buenoa C, Santos JFD, Huber N, Hage Jr E (2011) On the feasibility of friction spot joining in magnesium/fiber-reinforced polymer composite hybrid structures. Mater Sci Eng A 528:3841–3848
28. Esteves JV, Goushegir SM, Santos JFD, Canto LB, Hage Jr E, Amancio-Filho ST (2015) Friction spot joining of aluminum AA6181-T4 and carbon fiber-reinforced poly (phenylene sulfide): effects of process parameters on the microstructure and mechanical strength. Mater Des 66:437–445
29. Goushegir SM, Santos JFD, Amancio-Filho ST (2016) Failure and fracture micro-mechanisms in metal-composite single lap joints produced by welding-based joining techniques. Compos Pt A-Appl Sci Manuf 81:121–128
30. Balle F, Wagner G, Eifler D (2007) Ultrasonic spot welding of aluminum sheet/carbon fiber reinforced polymer-joints. Mater Werkst 38:934–938
31. Balle F, Wagner G, Eifler D (2009) Ultrasonic metal welding of aluminium sheets to carbon fibre reinforced thermoplastic composites. Adv Eng Mater 11:35–39
32. Balle F, Huxhold S, Wagner G, Eifler D (2011) Damage monitoring of ultrasonically welded aluminum/CFRP-joints by electrical resistance measurements. Procedia Eng 10:433–438
33. Pramanik A, Basak AK, Dong Y, Sarker PK, Uddin MS, Littlefair G, Dixit AR, Chattopadhyaya S (2017) Joining of carbon fibre reinforced polymer (CFRP) composites and aluminium alloys-a review. Compos Pt A-Appl Sci Manuf 101:1–29

Publisher's Note